

Article

Reduced Graphene Oxide Supported Zinc Tungstate Nanoparticles as Proficient Electro-Catalysts for Hydrogen Evolution Reactions

Norah Alhokbany *, Tansir Ahamad, Saad M. Alshehri and Jahangeer Ahmed *

Department of Chemistry, College of Science, King Saud University, Riyadh 11451, Saudi Arabia; tahamed@ksu.edu.sa (T.A.); alshehri@ksu.edu.sa (S.M.A.)

* Correspondence: nhokbany@ksu.edu.sa (N.A.); jahmed@ksu.edu.sa (J.A.)

Abstract: The nanocomposites of reduced graphene oxide (rGO) supported zinc tungstate nanoparticles (ZnWO_4 -NPs) receive considerable attention in electro-catalytic hydrogen evolution reactions (HER) and reveal significantly higher electro-catalytic performances than pure ZnWO_4 -NPs in alkaline media (i.e., 0.5 M KOH electrolyte). The polarization studies show that the ZnWO_4 -NPs@rGO nanocomposites exhibit low energy loss and good electrode stability during electrochemical reactions for HER. Furthermore, the Tafel slope of ZnWO_4 -NPs@rGO nanocomposites is found to be approximately 149 mV/dec, which closely agrees with the reported Tafel values of the noble metal electrocatalyst. In contrast, the performance of the ZnWO_4 -NPs@rGO nanocomposite is found to be approximately 1.5 times higher than that of ZnWO_4 -NPs in hydrogen production efficiency. Our results emphasize the significance of the nanocomposites with enhanced electro-catalytic activities by lowering the energy loss during electro-catalysis in an alkaline medium.

Keywords: nanocomposites; hydrogen evolution; energy storage and conversion



Citation: Alhokbany, N.; Ahamad, T.; Alshehri, S.M.; Ahmed, J. Reduced Graphene Oxide Supported Zinc Tungstate Nanoparticles as Proficient Electro-Catalysts for Hydrogen Evolution Reactions. *Catalysts* **2022**, *12*, 530. <https://doi.org/10.3390/catal12050530>

Academic Editor: Detlef W. Bahnemann

Received: 5 April 2022

Accepted: 7 May 2022

Published: 9 May 2022

Publisher's Note: MDPI stays neutral with regard to jurisdictional claims in published maps and institutional affiliations.



Copyright: © 2022 by the authors. Licensee MDPI, Basel, Switzerland. This article is an open access article distributed under the terms and conditions of the Creative Commons Attribution (CC BY) license (<https://creativecommons.org/licenses/by/4.0/>).

1. Introduction

Renewable energy is of current research interest among scientists in the energy conversion process. Transition metal oxides have recently been shown to possess potential in electrocatalytic hydrogen evolution reactions (HER). Hydrogen energy has fascinated the world as the most promising clean and renewable energy technology. Hydrogen evolution reaction (HER) via water electrolysis is a profitable strategy in the clean energy conversion process for fuel cell devices [1]. The transformation of solar energy to chemical energy is one of the ways to produce clean energy, but in this paper, we have focused on the electro-catalysis of water to HER [2–4]. Electrochemically active and low-cost electrode materials follow the given reaction process at the cathode for HER in alkaline media ($2\text{H}_2\text{O} + 2\text{e}^- \rightarrow \text{H}_2 + 2\text{OH}^-$) [5]. The most common electro-catalysts for gas evolution reactions are noble metal-based electrocatalysts. Noble metals such as Pt, Ru, and Ir-based electro-catalysts are also reported as well-organized electro-catalysts in HER [6–9]. However, the disadvantages of these catalysts are their scarce nature and very high cost. Therefore, it is very important to design low-cost, stable, and well-performed HER electrodes. However, scientists have been working worldwide to develop cost-effective and highly efficient electrode materials of clean energy technologies for commercialization. Recently, carbon-based nanocomposites are advanced materials used as electrocatalyst, photocatalyst, and electrode materials for energy storage devices [10–12]. Pt/rGO nanocomposites were reported as superior electro-catalysts over Pt nanoparticles for high HER activity in the acidic medium due to their excellent conductivity and surface area of rGO [13]. The Tafel slopes of Pt/GCE, Pt/rGO/GCE, and Pd/rGO electrodes for HER were reported to be of ~90, ~33, and ~154 mV/dec, respectively [13,14]. Graphene anchored Ag/cobalt ferrite nanoparticles were also reported as efficient electrode materials for electrochemical applications [15]. On

the other hand, tungstate [16–19], molybdate [20–23], ferrites [24,25], and delafossites [26] materials were also reported as proficient HER/OER/ORR electro-catalysts in clean energy applications. Heteroatoms doped carbon-based materials were recently reported as efficient electrocatalysts in water-splitting reactions [25,27]. Carbon-coated iron nanoparticles were reported as sustainable and non-precious trifunctional electro-catalysts, including HER catalysts in alkaline and acidic media [28]. Sulfide/carbides/nitrides based nanostructured materials as HER electrocatalysts were efficiently used in water electrolysis under acidic or basic media [22,29–31]. The hetero-structured materials were also reported as efficient electro-catalysts in water-splitting reactions [32–34]. It is noteworthy that nanocomposite materials with rGO show better electrical properties due to the high surface area and good thermal and chemical stability of rGO. Hence, the nanocomposite electrode materials perform well for HER. Hydrothermally synthesized tungstate nanorods have been recently reported as sensors with comprehensive performance [35]. The photo-catalysts have also produced hydrogen via solar water splitting reactions [36–38]. Subsequently, one of the key tasks could be an environmentally friendly approach to developing low-cost electrode materials for sustainable and clean energy with desirable performances. This study mainly delivers the conceivable electro-catalytic performance of ZnWO₄-NPs@rGO nanocomposites to HER via electro-chemical water-splitting reaction as a clean energy resource for fuel cell applications.

2. Results and Discussion

The electron microscopic studies (FESEM and TEM) were used to recognize the morphology and size of the prepared nanocomposites. The FESEM micrograph reveals that the prepared nanocomposites show well-defined ZnWO₄-NPs supported by rGO sheets (Figure 1a). The inset of Figure 1a shows high magnification FESEM micrographs for morphological analysis. The TEM study confirmed that ZnWO₄-NPs with an average diameter of ~50 nm are supported by rGO sheets (Figure 1b). The inset of Figure 1b shows the high resolution TEM (HRTEM) micrographs. The HRTEM study shows the <111> plane of the lattice fringes of monoclinic ZnWO₄-NPs. Figure 1c shows the XRD patterns of the ZnWO₄-NPs and the ZnWO₄-NPs@rGO nanocomposites. The XRD patterns demonstrated that the ZnWO₄ nanoparticles are recognized in the monoclinic structure, with a crystalline phase of reduced graphene oxide (rGO) appearing at two theta of 26.40°. The XRD patterns were indexed with JCPDS # 15-774 of ZnWO₄. Figure 1d shows the N₂ adsorption-desorption isotherm of ZnWO₄-NPs@rGO nanocomposites. The ZnWO₄-NPs@rGO nanocomposites exhibit a type IV adsorption-desorption isotherm [39,40]. The BET surface area of ZnWO₄-NPs@rGO was recorded (~118 m²/g) to be approximately nine times higher than pure ZnWO₄-NPs, as also reported elsewhere [41]. A high surface area is an important tool in electrochemical hydrogen evolution reactions via water-splitting reactions. Figure 2 shows the selected area FESEM-elemental mapping analysis of the ZnWO₄-NPs@rGO nanocomposites. This elemental mapping analysis confirmed the presence of Zn, W, O, and C elements in the nanocomposites, as shown in different colors. XPS was carried out to investigate the chemical states of the elements, i.e., Zn, W, O, and C, in ZnWO₄-NPs@rGO nanocomposites. The XPS spectrum of Zn (2p) shows two peaks at 1024.75 eV and 1048.73 eV of Zn2p_{3/2} and Zn2p_{1/2}, respectively, which confirmed that Zn is present in the Zn²⁺ chemical state (Figure 3a). The XPS spectrum of W (4f) displays two doublet peaks at 35.09 eV and 37.30 eV that will be represented to W4f_{7/2} and W4f_{5/2}, respectively, of the W⁶⁺ chemical state (Figure 3b). The XPS spectrum of O (1s) is shown in Figure 3c. The deconvoluted peaks confirmed the appearance of two types of oxygen atoms, i.e., one is due to the metal oxide at ~532.8 eV, and other one belongs to the functional group present in the graphene oxide matrix at ~533.7 eV. The XPS spectrum of C (1s) shows a peak at ~286.70 eV, which is deconvoluted into three peaks, i.e., peaks of C=C at ~285 eV, C-C at ~286 eV, and C-O at ~289 eV. The discussed characterization methods are enough to characterize the final products for further studies. We have used the prepared nanocomposites as the electro-catalysts for hydrogen evolution reactions (HERs) in alkaline media.

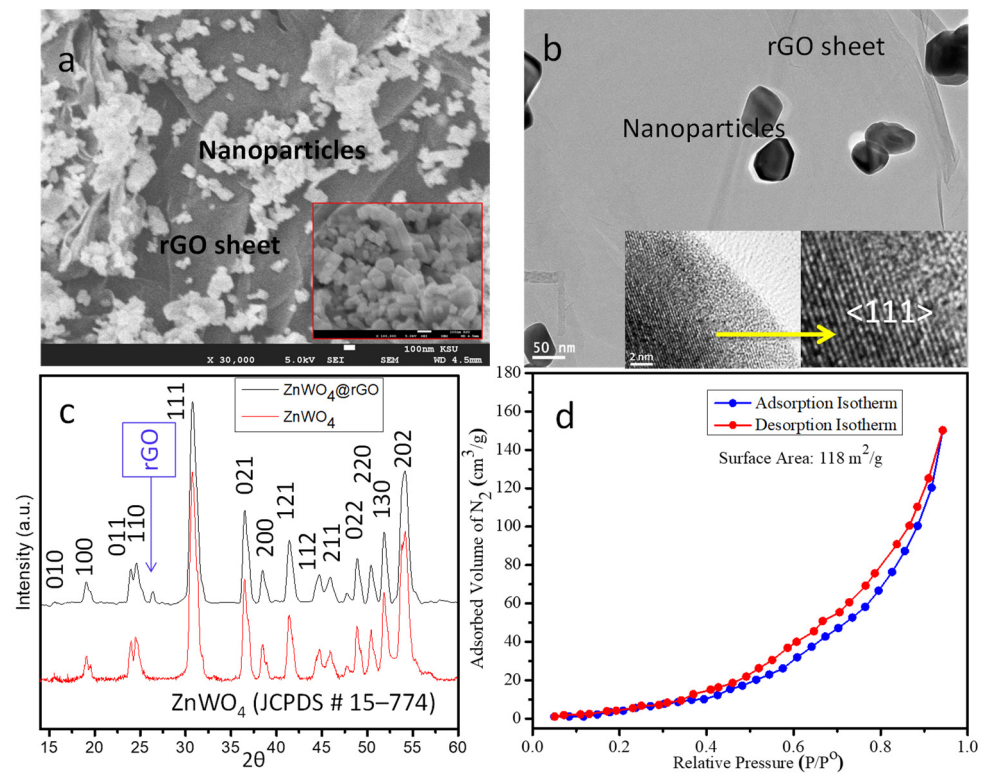


Figure 1. (a) FESEM (scale bar = 100 nm), (b) TEM, (c) XRD, and (d) N₂ adsorption–desorption isotherm of ZnWO₄-NPs@rGO nanocomposites. The inset of (a,b) shows high magnification FESEM and HR-TEM images, respectively.

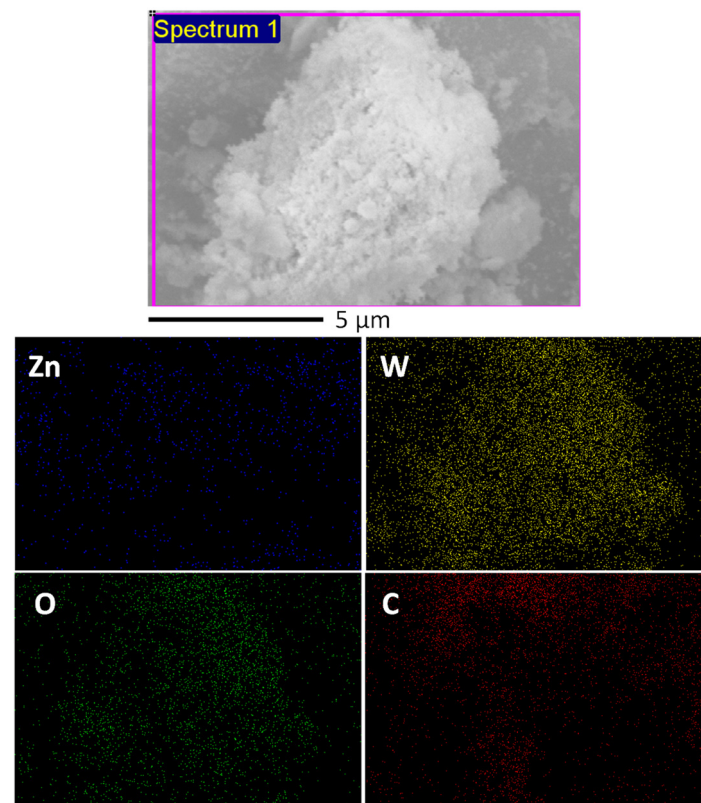


Figure 2. Elemental mapping analysis of the ZnWO₄-NPs@rGO nanocomposites.

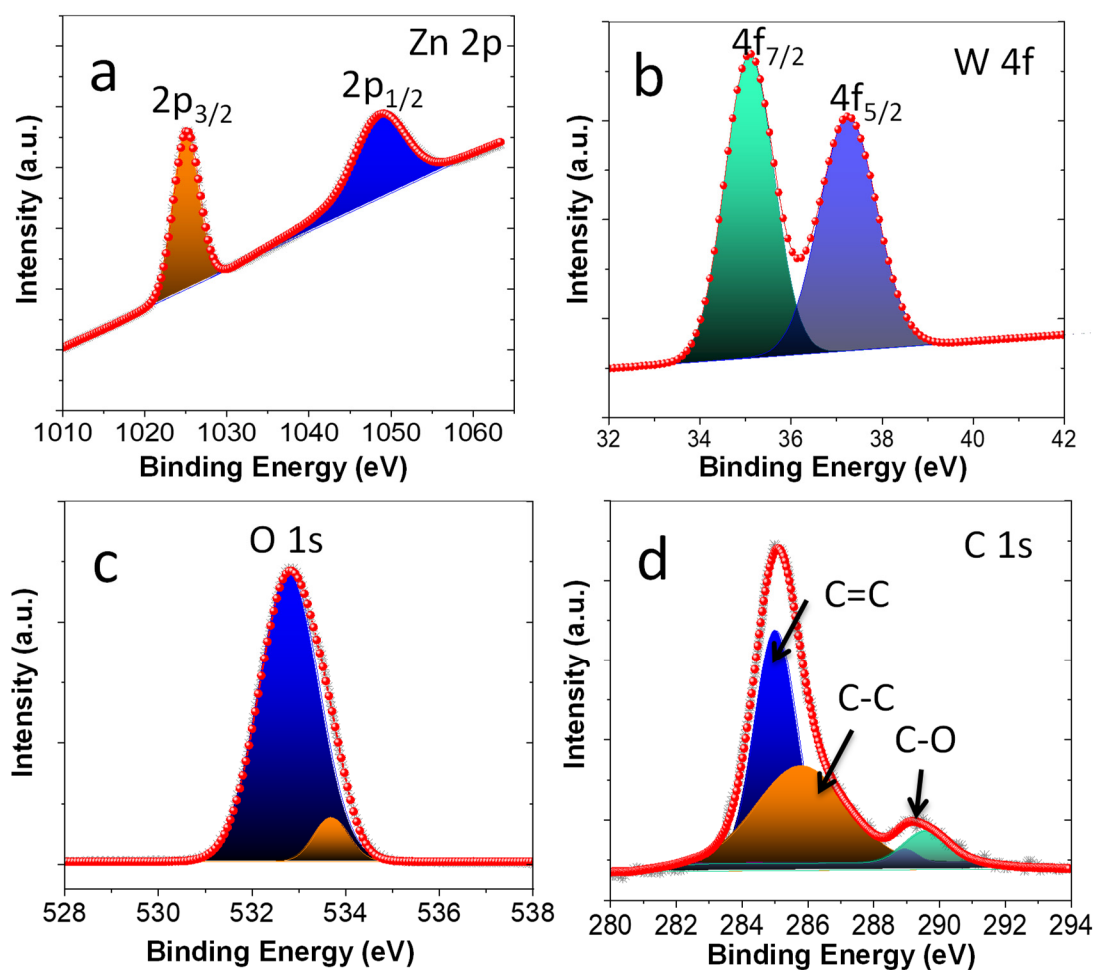


Figure 3. High resolution XPS spectra of (a) Zn 2p, (b) W 4f, (c) O 1s, and (d) C 1s.

The electro-catalytic HER performances of the prepared ZnWO₄-NPs@rGO nanocomposites have been investigated and also compared with the electro-catalytic performances of pure ZnWO₄-NPs. The electro-catalytic HER performances of the ZnWO₄-NPs@rGO nanocomposites and pure ZnWO₄-NPs were tested in 0.5 M KOH with a three-electrode electrochemical system at room temperature. CV and LSV polarization experiments were conducted at 25 mV/s from 0.0 V to −2.0 V versus Ag/AgCl for HER. Figure 4a shows the CV plots of ZnWO₄-NPs@rGO nanocomposites and pure ZnWO₄-NPs. The CV studies reveal that both ZnWO₄-NPs@rGO nanocomposites and pure ZnWO₄-NPs show HER activities in an alkaline medium, but, we have noted that the ZnWO₄-NPs@rGO nanocomposites show better HER activity than the pure ZnWO₄-NPs, as expected. Figure 4b shows the LSV polarization plots of ZnWO₄-NPs@rGO nanocomposites and ZnWO₄-NPs. The LSV studies confirm the HER activities of the ZnWO₄-NPs@rGO nanocomposites and pure ZnWO₄-NPs in the cathodic region and strongly support the CV results. From the CV and LSV results, the current densities were ~19 and ~12 mA/cm² of the ZnWO₄-NPs@rGO nanocomposites and pure ZnWO₄-NPs, respectively, at 25 mV/s. It is remarkable that the ZnWO₄-NPs@rGO nanocomposites show better electro-catalytic HER efficiency than the ZnWO₄-NPs. The onset over-potential of the ZnWO₄-NPs@rGO nanocomposites was found to be approximately 205 mV, which is better than that of the pure ZnWO₄-NPs (i.e., ~315 mV). The Tafel plots of the ZnWO₄-NPs@rGO nanocomposites and pure ZnWO₄-NPs are shown in Figure 4c. The Tafel slopes are found to be ~149 mV/dec and ~235 mV/dec of the ZnWO₄-NPs@rGO nanocomposites and pure ZnWO₄-NPs, respectively, at 25 mV/s. The Tafel slope of the Pt/GCE electrode for HER was reported to be ~90 mV/dec [13]. The Tafel slope of the Pd/rGO electrode was reported to be of ~154 mV/dec for HER [14].

The Tafel slopes of the NiMoO₄ and ZnMoO₄ nanostructured materials were reported to be ~133 mV/dec and ~230 mV/dec for HER in 0.5 M KOH [20,42]. It should be noted that the low onset potentials and low Tafel slope values with good stability indicate that ZnWO₄-NPs@rGO nanocomposite is a better HER electro-catalyst than pure ZnWO₄-NPs. It is also noteworthy that the Tafel value of the prepared ZnWO₄-NPs@rGO nanocomposites is consistent with the reported Tafel value of the expensive Pt-electrocatalyst [13]. The CA experiments also determined the electro-catalytic HER activity and stability of the electrodes containing ZnWO₄-NPs@rGO nanocomposites and pure ZnWO₄-NPs. The CA studies were investigated at a fixed cathodic potential of -1.65 V for 4 h (Figure 4d). The CA curves of the ZnWO₄-NPs@rGO nanocomposites show a higher current density with stability than the pure ZnWO₄-NPs for HER in 0.5 M KOH. These electro-catalytic results reveal the stable nature of the electrodes with efficient electro-catalytic HER performance. Therefore, we claim that the ZnWO₄-NPs@rGO nanocomposite has the potential to be one of the worthwhile HER electro-catalysts for energy conversion technologies.

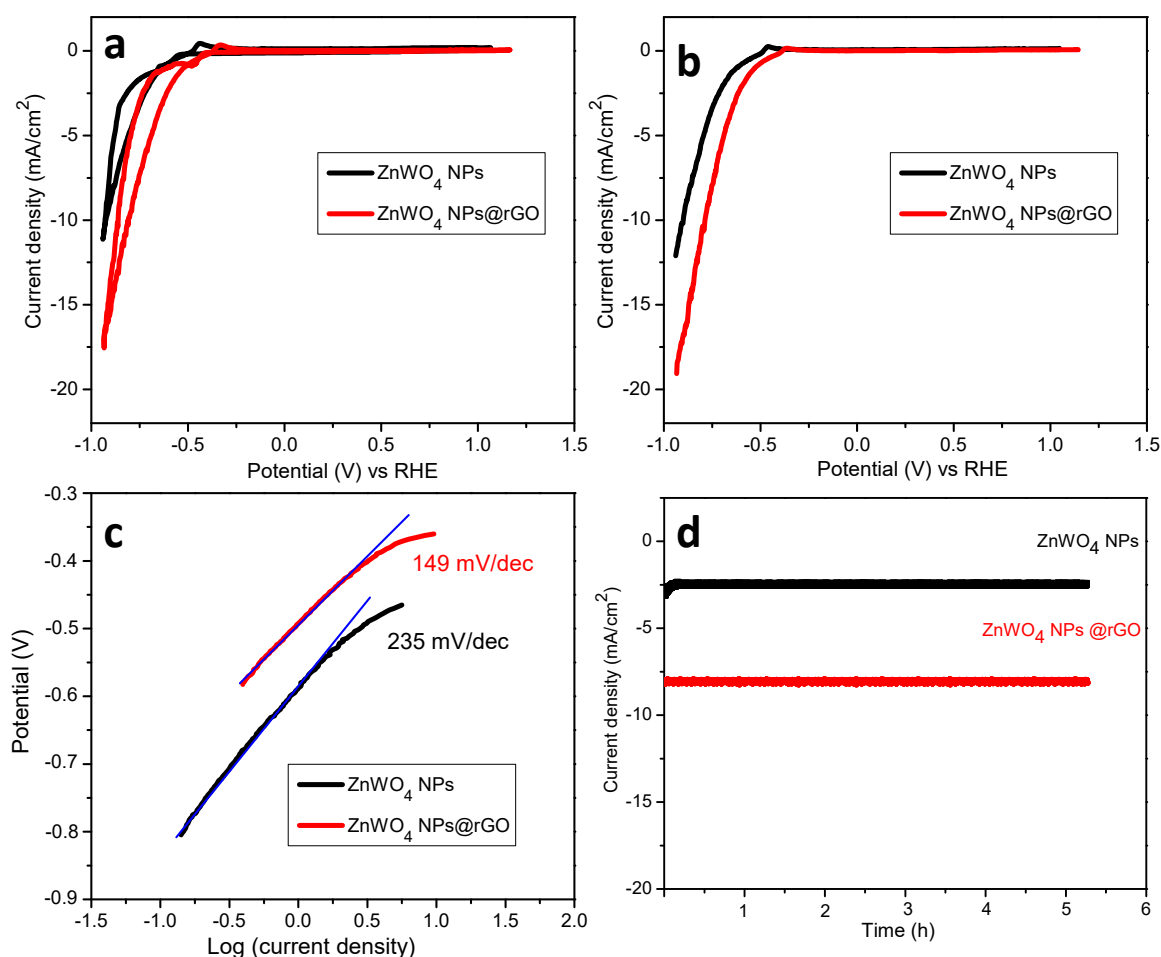


Figure 4. (a) CV, (b) LSV, (c) Tafel, and (d) CA curves of ZnWO₄-NPs@rGO nanocomposites and pure ZnWO₄-NPs for HER in 0.5 M KOH.

The gas generated during the electrolysis was also analyzed with an Agilent 7820A gas chromatograph equipped with a Molesieve GC column (30 m × 0.53 mm × 25 μm) and a thermal conductivity detector thermostatted at 40 °C for the detection of hydrogen (H₂). Argon was used as the carrier gas. The potentiostatic cathodic electrolysis was operated by maintaining a catalyst-loaded glassy carbon electrode at -1.65 V for 240 min in 0.5 M KOH solutions. Then, 100 μL aliquots of gas were collected from the headspace of the electrochemical cell over 20 min intervals with a gas-tight Hamilton syringe. The Faradic

efficiency of the HER catalysts is defined as the ratio of the amount of experimentally determined H_2 to that of the theoretically expected H_2 from the reaction. The catalytic activity of $ZnWO_4$ -NPs and $ZnWO_4$ -NPs@rGO nanocomposite for H_2 production was determined at a fixed cathodic potential of -1.65 V for 180 min. As shown in Figure 5a, the H_2 production efficiency of both the $ZnWO_4$ -NPs and $ZnWO_4$ -NPs@rGO nanocomposites is almost linear and increasing with time in the 0.5 M KOH solution and was found to be 95.68 mL/cm² after 180 min, which is higher than that of $ZnWO_4$ -NPs (64.27 mL/cm²). Figure 5b shows the hydrogen production per hour, and the $ZnWO_4$ -NPs@rGO nanocomposite shows 31.36 mL/cm².h, which is about 1.5 times higher than that of pristine $ZnWO_4$ -NPs. Furthermore, a 92–93% Faradic efficiency was obtained under alkaline conditions, suggesting the current density is directly related to hydrogen generation.

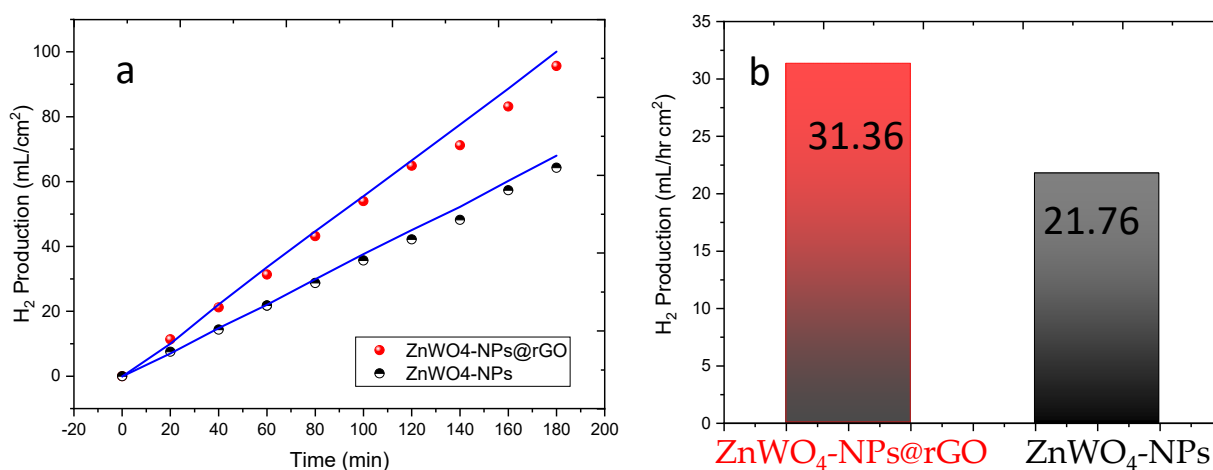


Figure 5. (a,b) Electro-catalytic H_2 production efficiency of $ZnWO_4$ -NPs@rGO nanocomposites and $ZnWO_4$ -NPs.

3. Experimental

$ZnWO_4$ -NPs and $ZnWO_4$ -NPs@rGO nanocomposites were prepared by following the previous reports [43]. The $ZnWO_4$ -NPs have been synthesized using the molten salts method. $Zn(NO_3)_2 \cdot 6H_2O$, $Na_2WO_4 \cdot 2H_2O$, $NaNO_3$, and KNO_3 reagents were taken in mortar pastel with a molar ratio of 1:1:40:40, respectively, and homogeneously hand grounded for 30 min. Thereafter, the homogenous mixture was transferred into a crucible and then placed in a muffle furnace at 500 °C for 5 h. The resulting material was washed several times using de-ionized water for the removal of inorganic moieties. The collected white colored powder was dried at 60 ± 5 °C. $ZnWO_4$ -NPs@rGO nanocomposites were synthesized by taking commercially available rGO and synthesized $ZnWO_4$ -NPs materials in 1:10 weight fractions along with 2.5 mL of ethylene glycol and 17.5 mL of de-ionized water followed by ultra-sonication for 15 min. This suspension was further treated hydrothermally at 120 °C/48 h to obtain the dark grey colored $ZnWO_4$ -NPs@rGO nanocomposites. Powder X-ray diffraction (PXRD, Bruker D-8 Advanced Diffractometer), a transmission electron microscope (TEM, JEOL, JSM-2100F, Japan), a field emission scanning electron microscope (FESEM, JEOL, JSM-7600F), and elemental mapping techniques were used to characterize the synthesized nanocomposites. Brunauer–Emmett–Teller (BET) measurements (V-Sorb 2800 Porosimetry Analyser) were conducted to estimate the surface area of the materials. X-ray photoelectron spectroscopy (XPS) data were collected on a PHI5300 spectrometer. Electro-catalytic studies of freshly prepared $ZnWO_4$ -NPs@rGO nanocomposites and pure $ZnWO_4$ -NPs were investigated with three electrodes configured with a CHI-660E electrochemical workstation using alkaline electrolyte at room temperature. The glassy carbon (0.07 cm²) was used as the working electrode, and an Ag/AgCl electrode was used as a reference electrode. KOH (0.5 M) was used as an electrolyte solution in the electrochemical studies of $ZnWO_4$ -NPs@rGO nanocomposites. Thus, we have measured the potential

against Ag/AgCl, but the electrode potential can be converted to RHE using the given equation, i.e., $E(\text{RHE}) = E(\text{Ag}/\text{AgCl}) + 0.197\text{V} + 0.059 \times \text{pH}$. Polarization studies were carried out using cyclic voltammetry (CV) and linear sweep voltammetry (LSV) at a scan rate of 25 mV s^{-1} . The chronoamperometry (CA) method was performed at a constant potential of -1.60 V to study the current stability.

4. Conclusions

ZnWO₄-NPs@rGO nanocomposites show better electro-catalytic HER performances than pure ZnWO₄-NPs in an alkaline medium (0.5M KOH). The polarization studies confirmed that ZnWO₄-NPs@rGO nanocomposites exhibit a lower onset over-potential (~205 mV) and Tafel slope (~149 mV/dec) than pure ZnWO₄-NPs in electrochemical water splitting to HER. ZnWO₄-NPs@rGO nanocomposite shows approximately 1.5 times higher hydrogen production efficiency than ZnWO₄-NPs. Hence, we can conclude that ZnWO₄-NPs@rGO nanocomposites could be considered one of the highly effective HER electro-catalysts for clean energy applications.

Author Contributions: N.A., Conceptualization, Data curation, Methodology, Formal analysis, Writing—Original draft preparation; T.A., Conceptualization, Methodology, Validation; S.M.A., Supervision, Resources, Project administration; J.A., Investigation, Validation, Project administration, Writing—review & editing. All authors have read and agreed to the published version of the manuscript.

Funding: Researchers Supporting Project number (RSP-2021/29), King Saud University.

Acknowledgments: The authors extend their sincere appreciation to the Researchers Supporting Project (RSP-2021/29) at the King Saud University, Riyadh, Saudi Arabia.

Conflicts of Interest: We state that the authors have no conflict of interest with this research.

References

1. McCrory, C.C.L.; Jung, S.; Ferrer, I.M.; Chatman, S.M.; Peters, J.C.; Jaramillo, T.F. Benchmarking Hydrogen Evolving Reaction and Oxygen Evolving Reaction Electrocatalysts for Solar Water Splitting Devices. *J. Am. Chem. Soc.* **2015**, *137*, 4347–4357. [[CrossRef](#)] [[PubMed](#)]
2. Wang, J.; Sun, Y.; Fu, L.; Sun, Z.; Ou, M.; Zhao, S.; Chen, Y.; Yu, F.; Wu, Y. A defective g-C₃N₄/RGO/TiO₂ composite from hydrogen treatment for enhanced visible-light photocatalytic H₂ production. *Nanoscale* **2020**, *12*, 22030–22035. [[CrossRef](#)] [[PubMed](#)]
3. Chen, X.; Zhao, J.; Li, G.; Zhang, D.; Li, H. Recent advances in photocatalytic renewable energy production. *Energy Mater.* **2022**, *2*, 200001. [[CrossRef](#)]
4. Wang, J.; Sun, Y.; Lai, J.; Pan, R.; Fan, Y.; Wu, X.; Ou, M.; Zhu, Y.; Fu, L.; Shi, F.; et al. Two-dimensional graphitic carbon nitride/N-doped carbon with a direct Z-scheme heterojunction for photocatalytic generation of hydrogen. *Nanoscale Adv.* **2021**, *3*, 6580–6586. [[CrossRef](#)]
5. Ren, S.; Duan, X.; Ge, F.; Zhang, M.; Zheng, H. Trimetal-based N-doped carbon nanotubes arrays on Ni foams as self-supported electrodes for hydrogen/oxygen evolution reactions and water splitting. *J. Power Sources* **2020**, *480*, 228866. [[CrossRef](#)]
6. Ahmed, J.; Mao, Y. Ultrafine Iridium Oxide Nanorods Synthesized by Molten Salt Method toward Electrocatalytic Oxygen and Hydrogen Evolution Reactions. *Electrochim. Acta* **2016**, *212*, 686–693. [[CrossRef](#)]
7. Du, N.; Wang, C.; Wang, X.; Lin, Y.; Jiang, J.; Xiong, Y. Trimetallic TriStar Nanostructures: Tuning Electronic and Surface Structures for Enhanced Electrocatalytic Hydrogen Evolution. *Adv. Mater.* **2016**, *28*, 2077–2084. [[CrossRef](#)]
8. Li, C.; Baek, J.-B. Recent Advances in Noble Metal (Pt, Ru, and Ir)-Based Electrocatalysts for Efficient Hydrogen Evolution Reaction. *ACS Omega* **2019**, *5*, 31–40. [[CrossRef](#)]
9. Li, J.; Hu, J.; Zhang, M.; Gou, W.; Zhang, S.; Chen, Z.; Qu, Y.; Ma, Y. A fundamental viewpoint on the hydrogen spillover phenomenon of electrocatalytic hydrogen evolution. *Nat. Commun.* **2021**, *12*, 3502. [[CrossRef](#)]
10. Asaithambi, S.; Sakthivel, P.; Karuppaiah, M.; Yuvakkumar, R.; Velauthapillai, D.; Ahamad, T.; Khan, M.A.M.; Mohammed, M.K.A.; Vijayaprabhu, N.; Ravi, G. The bifunctional performance analysis of synthesized Ce doped SnO₂/g-C₃N₄ composites for asymmetric supercapacitor and visible light photocatalytic applications. *J. Alloys Compd.* **2021**, *866*, 158807. [[CrossRef](#)]
11. Khalaf, N.; Ahamad, T.; Naushad, M.; Al-Hokbany, N.; Al-Saedi, S.I.; Almotairi, S.; Alshehri, S.M. Chitosan polymer complex derived nanocomposite (AgNPs/NSC) for electrochemical non-enzymatic glucose sensor. *Int. J. Biol. Macromol.* **2019**, *146*, 763–772. [[CrossRef](#)] [[PubMed](#)]
12. Ahamad, T.; Naushad, M.; Al-Saedi, S.I.; Almotairi, S.; Alshehri, S.M. Fabrication of MoS₂/ZnS embedded in N/S doped carbon for the photocatalytic degradation of pesticide. *Mater. Lett.* **2020**, *263*, 127271. [[CrossRef](#)]

13. Ghasemi, S.; Hosseini, S.R.; Nabipour, S. Preparation of nanohybrid electrocatalyst based on reduced graphene oxide sheets decorated with Pt nanoparticles for hydrogen evolution reaction. *J. Iran. Chem. Soc.* **2018**, *16*, 101–109. [[CrossRef](#)]
14. Kayan, D.B.; Turunç, E. Bio-reduced GO/Pd nanocomposite as an efficient and green synthesized catalyst for hydrogen evolution reaction. *Int. J. Energy Res.* **2021**, *45*, 11146–11156. [[CrossRef](#)]
15. Khan, M.A.M.; Khan, W.; Ahamed, M.; Ahmed, J.; Al-Gawati, M.A.; Alhazaa, A.N. Silver-Decorated Cobalt Ferrite Nanoparticles Anchored onto the Graphene Sheets as Electrode Materials for Electrochemical and Photocatalytic Applications. *ACS Omega* **2020**, *5*, 31076–31084. [[CrossRef](#)] [[PubMed](#)]
16. Ahmed, J.; Ahamad, T.; Ubaidullah, M.; Al-Enizi, A.M.; Alhabarah, A.N.; Alhokbany, N.; Alshehri, S.M. rGO supported NiWO₄ nanocomposites for hydrogen evolution reactions. *Mater. Lett.* **2018**, *240*, 51–54. [[CrossRef](#)]
17. AlShehri, S.M.; Ahmed, J.; Ahamad, T.; Arunachalam, P.; Ahmad, T.; Khan, A. Bifunctional electro-catalytic performances of CoWO₄ nanocubes for water redox reactions (OER/ORR). *RSC Adv.* **2017**, *7*, 45615–45623. [[CrossRef](#)]
18. Ahmed, J.; Alhokbany, N.; Ahamad, T.; Alshehri, S.M. Investigation of enhanced electro-catalytic HER/OER performances of copper tungsten oxide@reduced graphene oxide nanocomposites in alkaline and acidic media. *New J. Chem.* **2021**, *46*, 1267–1272. [[CrossRef](#)]
19. Khan, M.; Kumar, S.; Ahamad, T.; Alhazaa, A. Enhancement of photocatalytic and electrochemical properties of hydrothermally synthesized WO₃ nanoparticles via Ag loading. *J. Alloys Compd.* **2018**, *743*, 485–493. [[CrossRef](#)]
20. Ahmed, J.; Ubaidullah, M.; Alhokbany, N.; Alshehri, S.M. Synthesis of ultrafine NiMoO₄ nano-rods for excellent electro-catalytic performance in hydrogen evolution reactions. *Mater. Lett.* **2019**, *257*, 126696. [[CrossRef](#)]
21. Zang, M.; Xu, N.; Cao, G.; Chen, Z.; Cui, J.; Gan, L.; Dai, H.; Yang, X.; Wang, P. Cobalt Molybdenum Oxide Derived High-Performance Electrocatalyst for the Hydrogen Evolution Reaction. *ACS Catal.* **2018**, *8*, 5062–5069. [[CrossRef](#)]
22. Kumar, R.; Rai, R.; Gautam, S.; De Sarkar, A.; Tiwari, N.; Jha, S.N.; Bhattacharyya, D.; Ganguli, A.K.; Bagchi, V. Nano-structured hybrid molybdenum carbides/nitrides generated in situ for HER applications. *J. Mater. Chem. A* **2017**, *5*, 7764–7768. [[CrossRef](#)]
23. Ahmed, J.; Alam, M.; Khan, M.A.M.; Alshehri, S.M. Bifunctional electro-catalytic performances of NiMoO₄-NRs@RGO nanocomposites for oxygen evolution and oxygen reduction reactions. *J. King Saud Univ. Sci.* **2021**, *33*, 101317. [[CrossRef](#)]
24. Zhang, J.; Shang, X.; Ren, H.; Chi, J.; Fu, H.; Dong, B.; Liu, C.; Chai, Y. Modulation of Inverse Spinel Fe₃O₄ by Phosphorus Doping as an Industrially Promising Electrocatalyst for Hydrogen Evolution. *Adv. Mater.* **2019**, *31*, e1905107. [[CrossRef](#)] [[PubMed](#)]
25. Alshehri, S.M.; Alhabarah, A.N.; Ahmed, J.; Naushad, M.; Ahamad, T. An efficient and cost-effective tri-functional electrocatalyst based on cobalt ferrite embedded nitrogen doped carbon. *J. Colloid Interface Sci.* **2018**, *514*, 1–9. [[CrossRef](#)] [[PubMed](#)]
26. Mao, L.; Mohan, S.; Mao, Y. Delafossite CuMnO₂ as an Efficient Bifunctional Oxygen and Hydrogen Evolution Reaction Electrocatalyst for Water Splitting. *J. Electrochem. Soc.* **2019**, *166*, H233–H242. [[CrossRef](#)]
27. Zhang, S.; Xia, W.; Yang, Q.; Kaneti, Y.V.; Xu, X.; Alshehri, S.M.; Ahamad, T.; Hossain, M.S.A.; Na, J.; Tang, J.; et al. Core-shell motif construction: Highly graphitic nitrogen-doped porous carbon electrocatalysts using MOF-derived carbon@COF heterostructures as sacrificial templates. *Chem. Eng. J.* **2020**, *396*, 125154. [[CrossRef](#)]
28. Ahsan, A.; Santiago, A.R.P.; Rodriguez, A.; Maturano-Rojas, V.; Alvarado-Tenorio, B.; Bernal, R.; Noveron, J.C. Biomass-derived ultrathin carbon-shell coated iron nanoparticles as high-performance tri-functional HER, ORR and Fenton-like catalysts. *J. Clean. Prod.* **2020**, *275*, 124141. [[CrossRef](#)]
29. Ao, K.; Wei, Q.; Daoud, W.A. MOF-Derived Sulfide-Based Electrocatalyst and Scaffold for Boosted Hydrogen Production. *ACS Appl. Mater. Interfaces* **2020**, *12*, 33595–33602. [[CrossRef](#)]
30. Hu, S.; Wang, S.; Feng, C.; Wu, H.; Zhang, J.; Mei, H. Novel MOF-Derived Nickel Nitride as High-Performance Bifunctional Electrocatalysts for Hydrogen Evolution and Urea Oxidation. *ACS Sustain. Chem. Eng.* **2020**, *8*, 7414–7422. [[CrossRef](#)]
31. Ojha, K.; Saha, S.; Kumar, B.; Hazra, K.S.; Ganguli, A.K. Controlling the Morphology and Efficiency of Nanostructured Molybdenum Nitride Electrocatalysts for the Hydrogen Evolution Reaction. *ChemCatChem* **2016**, *8*, 1218–1225. [[CrossRef](#)]
32. Wang, T.; Wang, P.; Zang, W.; Li, X.; Chen, D.; Kou, Z.; Mu, S.; Wang, J. Nanoframes of Co₃O₄-Mo₂N Heterointerfaces Enable High-Performance Bifunctionality toward Both Electrocatalytic HER and OER. *Adv. Funct. Mater.* **2022**, *32*, 2107382. [[CrossRef](#)]
33. Zhang, L.; Zhu, J.; Li, X.; Mu, S.; Verpoort, F.; Xue, J.; Kou, Z.; Wang, J. Nurturing the marriages of single atoms with atomic clusters and nanoparticles for better heterogeneous electrocatalysis. *Interdiscip. Mater.* **2022**, *1*, 51–87. [[CrossRef](#)]
34. Wang, T.; Wang, P.; Pang, Y.; Wu, Y.; Yang, J.; Chen, H.; Gao, X.; Mu, S.; Kou, Z. Vertically mounting molybdenum disulfide nanosheets on dimolybdenum carbide nanomeshes enables efficient hydrogen evolution. *Nano Res.* **2022**, *15*, 3946–3951. [[CrossRef](#)]
35. Yao, X.; Zhao, J.; Liu, J.; Wang, F.; Wu, L.; Meng, F.; Zhang, D.; Wang, R.; Ahmed, J.; Ojha, K. H₂S sensing material Pt-WO₃ nanorods with excellent comprehensive performance. *J. Alloys Compd.* **2021**, *900*, 163398. [[CrossRef](#)]
36. Tri, N.L.M.; Trung, D.Q.; Van Thuan, D.; Cam, N.T.D.; Al Tahtamouni, T.; Pham, T.-D.; Duc, D.S.; Tung, M.H.T.; Van Ha, H.; Thu, N.H.A.; et al. The advanced photocatalytic performance of V doped CuWO₄ for water splitting to produce hydrogen. *Int. J. Hydrogen Energy* **2020**, *45*, 18186–18194. [[CrossRef](#)]
37. Li, X.; Xu, H.; Luo, Q.; Kang, S.; Qin, L.; Li, G.; Yang, J. Facile preparation and highly efficient photocatalytic hydrogen evolution of novel Cu_xNi_y nanoalloy/graphene nanohybrids. *Sustain. Energy Fuels* **2017**, *1*, 548–554. [[CrossRef](#)]
38. Zhao, Z.; Wang, X.; Shu, Z.; Zhou, J.; Li, T.; Wang, W.; Tan, Y. Facile preparation of hollow-nanosphere based mesoporous g-C₃N₄ for highly enhanced visible-light-driven photocatalytic hydrogen evolution. *Appl. Surf. Sci.* **2018**, *455*, 591–598. [[CrossRef](#)]

39. Ahamad, T.; Naushad, M.; Alzahrani, Y.; Alshehri, S.M. Photocatalytic degradation of bisphenol-A with g-C₃N₄/MoS₂-PANI nanocomposite: Kinetics, main active species, intermediates and pathways. *J. Mol. Liq.* **2020**, *311*, 113339. [[CrossRef](#)]
40. Ubaidullah, M.; Al-Enizi, A.M.; Ahamad, T.; Shaikh, S.F.; Al-Abdrabalnabi, M.A.; Samdani, M.S.; Kumar, D.; Alam, M.A.; Khan, M. Fabrication of highly porous N-doped mesoporous carbon using waste polyethylene terephthalate bottle-based MOF-5 for high performance supercapacitor. *J. Energy Storage* **2020**, *33*, 102125. [[CrossRef](#)]
41. Alshehri, S.M.; Ahmed, J.; Ahamad, T.; Alhokbany, N.; Arunachalam, P.; Al-Mayouf, A.M.; Ahmad, T. Synthesis, characterization, multifunctional electrochemical (OGR/ORR/SCs) and photodegradable activities of ZnWO₄ nanobricks. *J. Sol-Gel Sci. Technol.* **2018**, *87*, 137–146. [[CrossRef](#)]
42. Ahmed, J.; Khan, M.M.; Alshehri, S.M. Zinc molybdenum oxide sub-micron plates as electro-catalysts for hydrogen evolution reactions in acidic medium. *Mater. Lett.* **2020**, *284*, 128996. [[CrossRef](#)]
43. Alhokbany, N.; Alshehri, S.M.; Ahmed, J. Synthesis, Characterization and Enhanced Visible Light Photocatalytic Performance of ZnWO₄-NPs@rGO Nanocomposites. *Catalysts* **2021**, *11*, 1536. [[CrossRef](#)]